



HAL
open science

Price impact in equity auctions: zero, then linear

Mohammed Salek, Damien Challet, Ioane Muni Toke

► **To cite this version:**

Mohammed Salek, Damien Challet, Ioane Muni Toke. Price impact in equity auctions: zero, then linear. 2023. hal-03938660v1

HAL Id: hal-03938660

<https://hal.science/hal-03938660v1>

Preprint submitted on 13 Jan 2023 (v1), last revised 18 Sep 2023 (v2)

HAL is a multi-disciplinary open access archive for the deposit and dissemination of scientific research documents, whether they are published or not. The documents may come from teaching and research institutions in France or abroad, or from public or private research centers.

L'archive ouverte pluridisciplinaire **HAL**, est destinée au dépôt et à la diffusion de documents scientifiques de niveau recherche, publiés ou non, émanant des établissements d'enseignement et de recherche français ou étrangers, des laboratoires publics ou privés.



Distributed under a Creative Commons Attribution - NonCommercial - NoDerivatives 4.0 International License

Price impact in equity auctions: zero, then linear

Mohammed Salek,^{*} Damien Challet,[†] and Ioane Muni Toke[‡]

*Université Paris-Saclay,
CentraleSupélec,
Laboratoire de Mathématiques et Informatique pour la Complexité et les Systèmes,
91192 Gif-sur-Yvette,
France*

(Dated: January 13, 2023)

Using high-quality data, we report several statistical regularities of equity auctions in the Paris stock exchange. First, the average order book density is linear around the auction price at the time of auction clearing and has a large peak at the auction price. The linear part comes from fast traders, while the peak is due to slow traders. The impact of a new market order or cancellation at the auction time can be decomposed into three parts as a function of the size of the additional order: (1) zero impact because of the discrete nature of prices; this holds for surprisingly large orders relative to the auction volume (2) linear impact for additional orders up to a large fraction of the auction volume (3) for even larger orders price impact is non-linear, frequently superlinear.

I. INTRODUCTION

Most electronic markets rely on auctions to start and end trading days in an orderly way. Because the volume involved during auctions is larger than the liquidity available at a given time in a typical open-market limit order book, auctions reduce price impact and fluctuations. The share of the closing auction in the total exchanged volume has significantly increased over the years (Blackrock, 2020), especially in European markets (Raillon, 2020). This increase highlights the importance of the auction mechanism in the price formation process.

In contrast to the abundant literature about open-market dynamics, work on auctions is scarce. On the theoretical side, Muni Toke (2015) derives the distribution of the exchanged volume and the auction price using a stochastic order flow model during a standard call auction. In the same vein, Derksen et al. (2020) propose a stochastic model for call auctions which produces a concave price impact function of market orders; in addition, Derksen et al. (2022) build on the previous model to demonstrate the heavy-tailed nature of price and volume in closing auctions. Besides, Donier and Bouchaud (2016) show that under sufficient regularity conditions (continuous price and time) and using a first-order Taylor expansion of supply and demand curves, price impact in Walrasian auctions is linear in the vicinity of the auction price.

Empirically, Pagano and Schwartz (2003) find that introducing opening and closing call auctions improves market quality and lowers execution costs in the Paris stock exchange. Boussetta et al. (2017) add that although opening volumes are decreasing and the market is fragmenting, the opening auction still improves market quality on Euronext Paris. They also report that slow brokers submit orders early, whereas high-frequency traders tend to act moments before the clearing. Challet and Gourianov (2018) analyze US equities data and compute the auction price response functions conditional on the addition, and cancellation of an order. In addition, Challet (2019) demonstrates that a strategic behavior of agents is needed to explain the antagonistic effects of activity acceleration and indicative price volatility decrease as the auction end approaches.

More recently, Jegadeesh and Wu (2022) assess the robustness of closing auctions by comparing the price impact between NASDAQ and NYSE exchanges and find that the cost of trading during closing auctions is generally smaller than during trading hours. They also find that closing auctions mainly attract uninformed and passive

^{*} mohammed.salek@centralesupelec.fr

[†] damien.challet@centralesupelec.fr

[‡] ioane.muni-toke@centralesupelec.fr

investors, while informed traders prefer to act during continuous market hours. In the same spirit, Besson and Fernandez (2021) analyze the closing auction in European markets and use a linear function to fit the impact of market orders; they report a smaller instantaneous impact for later submissions, and an overall cost of trading on close two to three times smaller than during trading hours.

Here, we characterize in detail the empirical properties of liquidity and price impact in equity auctions. We do not find a straightforward linear impact: while adding or canceling a market (or marketable) order at the auction time has a linear component, the discreteness of the limit order book mechanically leads to zero price impact for small enough orders. These free-of-cost volumes can represent a fairly large fraction of the total matched volume.

First, we introduce a discrete-price auction mathematical framework (Section II) suitable to derive the conditions under which price impact is zero or linear (Section V, Proposition 4). Next, we present the high-quality data used in this work: a large dataset from the European high-frequency financial (BEDOFIH) database (Section III). The main part of this paper consists in a detailed study of several statistical regularities of auctions (Sections IV and V):

1. in addition to a high peak of volumes at the auction price, each side (buy and sell) of the average limit order book has a skewed bell shape around the auction price and can be considered linear in the vicinity of the auction price;
2. breaking down the average limit order book densities by the agents' latency (HFT, MIXED, NON) and their account type (own account, client account, market maker, parent company, retail market organisation. . .) allows us to capture subtle aspects of limit orders placement for each category;
3. we relate the instantaneous price impact shape just after the clearing with latent models of market impact;
4. by computing the price impact function just before the auction clearing for a large number of stock-days, we show that zero-impact volumes could be rather large and —often— simultaneously in both directions (buying and selling).
5. thanks to a change point detection criterion, we characterize the precise range of volumes where additional market orders or cancellations result in a linear price impact for every day and asset;
6. we examine whether the expiry of listed derivatives affects the final price response of the closing auction, and show that the order book tends to be more resistant to price changes during expiry dates;
7. we investigate the evolution of price impact during the accumulation period.

II. A MATHEMATICAL FRAMEWORK FOR AUCTIONS

In Euronext markets, equity auctions start with an accumulation period and end with a clearing process. During the accumulation period, participants send their orders (quantity, price, side, order type, . . .) to the exchange. Types of orders include market orders, limit orders, activated stop orders, and valid for auction orders. Modifications and cancellations are allowed, but transactions cannot occur. At any time during the accumulation process and at the end of the auction, the price that maximizes the matched volume and minimizes the imbalance is computed. At the auction time, buy (resp. sell) orders whose prices are larger (resp. smaller) than the auction price are executed, while limit orders whose price equals the auction price may be matched or remain in the order book after the auction.

Definition 1 (Supply and demand). For an auction $\mathcal{A} = (a, d)$, where a is the auction type (open, close, . . .) at date d , we define the available supply $S(p, t)$ and demand $D(p, t)$ at a price p and time t as, dropping the (a, d) for the sake of clarity,

$$\begin{aligned} S(p, t) &= \sum_{p' \leq p} V_S(p', t), \\ D(p, t) &= \sum_{p' \geq p} V_B(p', t), \end{aligned} \tag{1}$$

where $V_S(p', t)$ (resp. $V_B(p', t)$) is the available sell volume (resp. buy volume) at a price p' and time t .

Limit orders can only be submitted on a discrete price grid. Therefore, at any time t , $p \mapsto S(p, t)$ is a non-decreasing right-continuous step function, and $p \mapsto D(p, t)$ is a non-increasing left-continuous step function.

Definition 2 (Auction price and volume). For an auction $\mathcal{A} = (a, d)$, the auction price p_a^d noted p_a is the price that maximizes the exchanged auction volume Q_a^d noted Q_a at the time of the clearing T_a^d noted T_a .

In this work we will always assume that supply $S(p, T_a)$ and demand $D(p, T_a)$ intersect, so that Q_a always exists and is unique. Note however that p_a is often not uniquely defined by the maximization of the exchanged volume alone; this is why exchanges implement a complementary set of rules such that p_a is always well defined. In the case of the Euronext markets used in this work, when multiple prices maximize the exchanged volume, the chosen p_a is the one with the smallest imbalance. Then, if multiple prices with the highest executable volume and the smallest imbalance coexist, the auction price is the one closest to the reference price (last traded price).

Definition 3 (Indicative price and volume). For an auction \mathcal{A} , the indicative price p_t^{ind} and the indicative volume Q_t^{ind} at time $t \leq T_a$ are the hypothetical auction price and the total matched volume if the clearing took place at time t .

Obviously, we have $p_a = p_{T_a}^{\text{ind}}$ and $Q_a = Q_{T_a}^{\text{ind}}$. From now on, the time notation will be omitted when we work at time $t = T_a$ (e.g., $S(p)$ stands for $S(p, T_a)$). Note however that subsequent definitions and results can be stated for any time $t \leq T_a$ using time-dependent notations and substituting p_a with p_t^{ind} and Q_a with Q_t^{ind} .

Proposition 1. Let \mathcal{A} be an auction with an auction price p_a and an auction volume Q_a . We have:

- (a) $Q_a = \max_p \min(S(p), D(p))$;
- (b) $p_a \in \{p \mid Q_a = \min(S(p), D(p))\}$.

Proof. For a given price p , buyers and sellers can exchange a volume equal to $\min(S(p), D(p))$ at most. \square

Definition 4 (Buy and sell densities). For an auction $\mathcal{A} = (a, d)$, we define the buy (resp. sell) density ρ_B^d (resp. ρ_S^d) at a price p as

$$\rho_{\bullet}^d(p) = \frac{V_{\bullet}(p)}{\delta p}, \quad \bullet \in \{B, S\}, \quad (2)$$

where δp is the difference between the price p and the next non-empty tick price when $\bullet = B$, and δp is the difference between p and the previous non-empty tick price when $\bullet = S$.

To define a meaningful average density over a large number of days, volumes can be scaled by the auction volume Q_a^d at day d , and prices can be substituted with log-price differences from the auction price $p \leftarrow \log(p/p_a)$.

Definition 5 (Scaled buy and sell densities). For an auction $\mathcal{A} = (a, d)$, we define the scaled buy and sell densities as

$$\tilde{\rho}_{\bullet}^d(x) = \frac{\rho_{\bullet}^d(p_a e^x)}{Q_a^d}, \quad \bullet \in \{B, S\}, \quad (3)$$

where $x = \log\left(\frac{p}{p_a}\right)$. Furthermore, if we substitute δp by a constant δx , we can compute for a given stock the average scaled density as

$$\langle \tilde{\rho}_{\bullet}(x) \rangle = \left\langle \frac{V_{\bullet}(p_a e^x)}{Q_a^d \times \delta x} \right\rangle, \quad \bullet \in \{B, S\}, \quad (4)$$

where the average is taken across time (days).

Observe that this quantity is a discrete version of the continuous marginal supply and demand curves defined in Donier and Bouchaud (2016), where $\rho_B(p) = -\partial_p D$ and $\rho_S(p) = \partial_p S$.

Definition 6 (Matched and remaining volumes). For an auction \mathcal{A} , we define $V_{\bullet}^M(p)$ as the matched (executed) volume at a price p and side \bullet , and $V_{\bullet}^R(p)$ as the remaining (non-executed) volume at a price p and side \bullet .

Obviously, for any price $p > p_a$, we have $V_B^M(p) = V_B(p)$, $V_S^M(p) = 0$, $V_B^R(p) = 0$, and $V_S^R(p) = V_S(p)$. Symmetrically, for any price $p < p_a$, we have $V_B^M(p) = 0$, $V_B^R(p) = V_B(p)$, $V_S^M(p) = V_S(p)$, and $V_S^R(p) = 0$. Consequently, $V_{\bullet}^M(p) \times V_{\bullet}^R(p)$ can be non-zero only if $p = p_a$.

Proposition 2. Let \mathcal{A} be an auction with an auction price p_a and an auction volume Q_a . The following equalities stand:

- (a) $V_{\bullet}(p) = V_{\bullet}^M(p) + V_{\bullet}^R(p)$, $\bullet \in \{B, S\}$, for any price p ;
- (b) $Q_a = S(p_a) - V_S^R(p_a) = D(p_a) - V_B^R(p_a)$;
- (c) $V_S^R(p_a) \times V_B^R(p_a) = 0$.

Proof. (a) and (b) are straightforward. (c) is proved by contradiction: if $V_S^R(p_a) \times V_B^R(p_a) \neq 0$, then $(V_S^R(p_a), V_B^R(p_a)) \neq (0, 0)$. This implies that a residual volume $\delta V = \min(V_S^R(p_a), V_B^R(p_a)) > 0$ can be matched between buyers and sellers at the auction price and thus contradicts the fact that Q_a is maximizing the exchanged volume during the auction. \square

Let us now introduce volumes scaled by the auction volume: given an integer volume of shares $q \in \mathbb{N}$, we define the scaled volume $\omega = q/Q_a$.

Definition 7 (Price impact). For an auction \mathcal{A} , for any $\omega > 0$, we define the price impact before the auction clearing of a buy (resp. sell) market order $I_B(\omega)$ (resp. $I_S(\omega)$) as the absolute change in the auction log-price immediately after submitting a buy (resp. sell) market order of size $q = \omega \times Q_a$

$$I_{\bullet}(\omega) = \left| \log \left(\frac{p_{\omega}}{p_a} \right) \right|, \quad \bullet \in \{B, S\}, \quad (5)$$

where p_{ω} is the new auction price after injecting the market order.

Proposition 3. Let \mathcal{A} be an auction with an auction price p_a and an auction volume Q_a . We inject a market order of size $q = \omega Q_a$ before the auction clearing. The new auction price is p_{ω} . We have:

- (a) The function $I_{\bullet} : \omega \mapsto \left| \log \left(\frac{p_{\omega}}{p_a} \right) \right|$, for $\bullet \in \{B, S\}$ and $\omega > 0$, is a non-decreasing and right-continuous step function.
- (b) Let $(\omega_B^{(i)})_{i \geq 0}$ be the ordered points of discontinuity of I_B . Then

$$\begin{aligned} \omega_B^{(0)} &= \frac{V_S^R(p_a) + V_B^M(p_a)}{Q_a}, \\ \omega_B^{(i)} &= \omega_B^{(i-1)} + \frac{V_S(p_B^{(i)}) + V_B(p_B^{(i)})}{Q_a}, \quad i \geq 1, \end{aligned} \quad (6)$$

where $p_B^{(i)} > p_a$ is the i^{th} non-empty price tick strictly greater than the auction price.

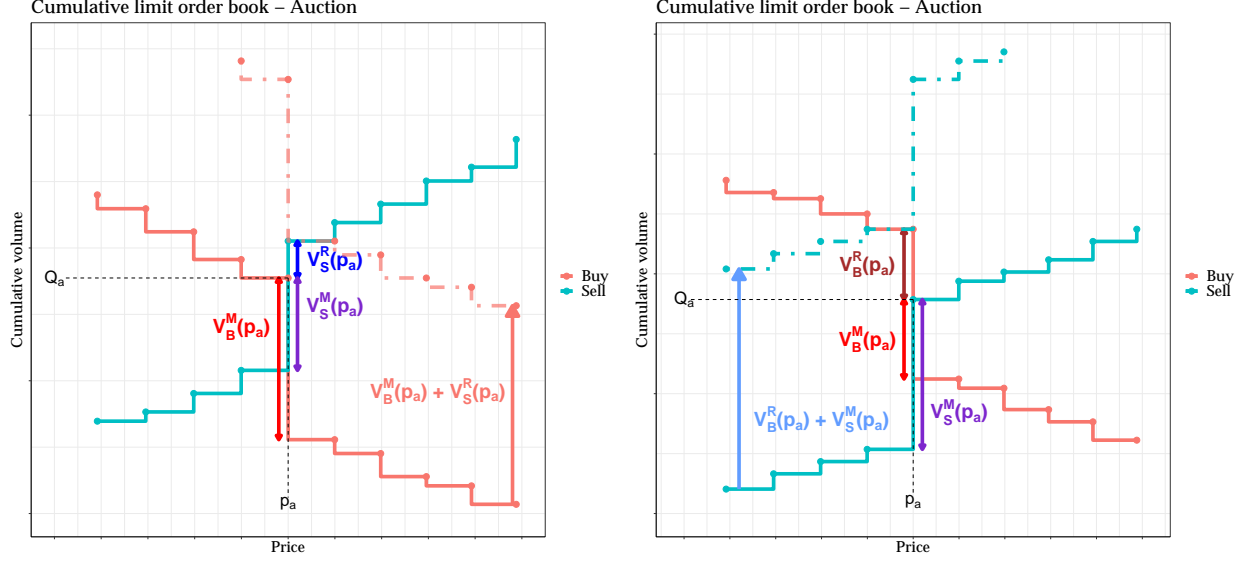


FIG. 1: Cumulative buy (red curves) and sell curves (blue curves) during hypothetical auctions. Left panel: the buy volume is totally matched at the auction price; right panel: the sell volume at the auction price is totally matched at the auction price. Dash-dotted lines: effect of an addition buy market order (left plot) and sell market order (right plot): the auction price can change only when the market order is larger than the matched volume plus the imbalance, which explains why zero impact is prevalent.

(c) Let $(\omega_S^{(i)})_{i \geq 0}$ be the ordered points of discontinuity of I_S . Then

$$\begin{aligned} \omega_S^{(0)} &= \frac{V_S^M(p_a) + V_B^R(p_a)}{Q_a}, \\ \omega_S^{(i)} &= \omega_S^{(i-1)} + \frac{V_S(p_S^{(i)}) + V_B(p_S^{(i)})}{Q_a}, \quad i \geq 1, \end{aligned} \quad (7)$$

where $p_S^{(i)} < p_a$ is the i^{th} non-empty price tick strictly lower than the auction price.

Obviously $I_\bullet(\omega_\bullet^{(i)}) = \left| \log(p_\bullet^{(i+1)}/p_a) \right|$. Also, remark that if all price ticks contain non null volume ($V_B + V_S > 0$), then $p_\bullet^{(i)} = p_a \pm i\theta$, where θ is the tick size. The proof of Proposition 3 is given in Appendix A. Proposition 3 allows us to compute the impact function at any time of a given auction, including during the accumulation period. In addition, the price impact of a new order is zero if its size is smaller than $\omega_\bullet^{(0)} Q_a$. Figure 1 provides a graphical explanation of $\omega_\bullet^{(0)}$ formulas. On the left panel for example, the buy volume at the auction price is totally matched ($V_B(p_a) = V_B^M(p_a)$ and $V_B^R(p_a) = 0$). In this case, in order to shift the price, a buyer would need to execute a market buy order of minimal volume $V_S^R(p_a) + V_B(p_a)$. Alternatively, a seller would need to execute a market sell order of minimal volume $V_S^M(p_a)$. The right panel of Figure 1 illustrates the symmetric case in which the sell volume at the auction price is totally matched ($V_S(p_a) = V_S^M(p_a)$ and $V_S^R(p_a) = 0$). Moreover, observe that if a trader sends a market order of exact size $q = \omega_\bullet^{(0)} \times Q_a \in \mathbb{N}$, then both p_a and $p_\bullet^{(1)}$ maximize the auction volume. As explained above, the new auction price would be the one with the smallest imbalance, i.e. equal remaining volumes. If p_a and $p_\bullet^{(1)}$ have equal imbalances, then the new auction price is the closest to the reference price. Here, we assumed that whenever $q = \omega_\bullet^{(0)} \times Q_a \in \mathbb{N}$, the price automatically shifts to $p_\bullet^{(1)}$.

Also, by Proposition 3, $V_S(p_\bullet^{(i)}) + V_B(p_\bullet^{(i)}) = Q_a \times (\omega_\bullet^{(i)} - \omega_\bullet^{(i-1)})$ for $i \geq 1$ is the necessary volume to take the price from $p_\bullet^{(i)}$ to $p_\bullet^{(i+1)}$. We therefore define $\delta\omega_\bullet^{(i)} = \omega_\bullet^{(i)} - \omega_\bullet^{(i-1)}$ for $i \geq 1$ to denote this scaled incremental

volume, with the convention that $\delta\omega_{\bullet}^{(0)} = \omega_{\bullet}^{(0)}$. Finally, notice that a cancellation of a buy market order of size q affects the price in the same way as submitting a sell market order of the same size: in both cases the new price p_{ω} is a solution of $S(p_{\omega}) + q = D(p_{\omega})$. Similarly, cancelling a sell market order has the same effect as submitting a buy market order. Consequently, we only focus on the price impact of market order submissions in the following.

III. DATA

The dataset used in this work is part of the BEDOFIH database (Base Européenne de Données Financières à Haute-fréquence) built by the European Financial Data Institute (EUROFIDAI). The dataset provides detailed order data for all stocks traded on Euronext Paris between 2013 and 2017. For each stock and each trading day, information is provided in four files:

- a history orders file that contains all the orders that remained in the central limit order book from the previous trading day ;
- a current orders file that contains all submissions, modifications, and cancellations for the current trading day ;
- a trades file that lists all the transactions that took place during the current trading day ;
- an events file that lists special market events, if any, such as a delayed opening, a halt in trading, etc.

In addition to standard information such as time with microsecond precision, price, side (buy/sell), quantity, and price threshold for stop orders, we have access to additional order details in these files, some of which are computed *ex-post*. These include the order type and its temporal validity (market, limit, valid-for-auction, valid-for-closing, etc.), the high-frequency status of the market participant (HFT, NON-HFT, or MIXED), and the account type (own account, client account, market maker, parent company, retail liquidity provider, retail market organization).

In order to reconstruct the exact state of the limit order book (LOB) at any point during the auction, we combine the information from the four different files for each stock and each trading day to create a snapshot. We select the 34 most traded stocks on Euronext Paris between 2013 and 2017 and analyze 2 to 5 years' worth of data for each stock, totaling $N = 34,977$ stock-days. A small number of these stock-days result in errors or mismatches (e.g., dataset errors, non-crossing supply and demand for the opening auction, or half-day trading/halted trading before 17:30 for the closing auction). After removing these invalid snapshots, we are left with $N_o = 34,971$ valid snapshots at the opening auction time and $N_c = 34,820$ valid snapshots at the closing auction time.

Using these reconstructed snapshots just before the auction time, we compute reconstructed prices and volumes as per Euronext rules, i.e., by maximizing the exchanged volume and minimizing the imbalance. This boils down to finding the intersection of the reconstructed supply and demand curves. Table I reports the percentage of snapshots for which the reconstructed price (resp. volume) matches the actual auction price (resp. volume) among valid snapshots. The remaining discrepancies may be a result of using simplified rules to account for stop orders and occasional contradictions between recorded data in the orders file and the trades file. For these few unmatched snapshots, we note that the discrepancies between computed and actual quantities are small: less than 1 basis point on the absolute average difference from the auction price and 0.2% on the absolute average distance from the auction volume. These few unmatched auctions are discarded from the sample in the subsequent analysis, though they would not alter the outcome of our experiments.

TABLE I: Percentages of auction snapshots with accurate reconstruction.

	Opening auction	Closing auction
Number of valid snapshots	34,971	34,820
% snapshots matching the auction price	99.6%	99.9%
% snapshots matching the auction volume	99.0%	99.7%
% snapshots matching both	98.9%	99.6%

IV. AVERAGE SHAPE OF THE AUCTION LIMIT ORDER BOOK

This section investigates the typical shape of the limit order book at time T_a of an equity auction, what it implies for post-clearing price impact, and how the average LOB shape can be broken down by latency and account type of market participants.

A. Pre-clearing vs. post-clearing LOB shape

For each stock of the dataset, we compute the buy and sell average empirical densities $\langle \tilde{\rho}_\bullet \rangle$ (see Definition 5) as a function of the log-price difference $x = \log\left(\frac{p}{p_a}\right)$. Figure 2 shows the average LOB density for the most traded stock in our dataset (ISIN FR0000120271, TTE.PA, TotalEnergies). We distinguish the orders that are cleared by the auction process (dotted lines) from the ones that remain in the LOB after the end of the auction (full lines). Average LOB densities are very similar across all the studied stocks.

Figure 2 shows the average LOB densities at the closing auction: the buy and sell densities have a skewed bell-shaped curve around the auction price. Opening and closing auctions have clearly different LOB densities. As expected, the average LOB density is noisier at the opening auction than at the closing auction which reflects the typical liquidity available at either auction (Challet, 2019). However, the following remarks hold for both auctions:

- there is a peak at the auction price, i.e. $\langle \tilde{\rho}_\bullet \rangle(0)$ is larger than typical values taken near 0. This translates an accumulation of orders on $p = p_a$ on average at the time of the clearing ;
- $\langle \tilde{\rho}_\bullet \rangle$ is linear around $x = 0$, i.e. $p = p_a$.

As shown by Fig. 2, all buy orders with $p > p_a$ are cleared, and all buy orders with $p < p_a$ remain in the LOB after the auction as long as their temporal validity extends beyond the clearing; similarly, all sell orders with $p < p_a$ are cleared and all sell orders with $p > p_a$ remain in the LOB after the auction. For $p = p_a$, some orders are matched, some are not. This explains why the peaks of buy and sell volumes at p_a are reduced after the clearing. Finally, the auction-only orders are removed from the LOB after the clearing if they are not executed.

B. Post-clearing instantaneous price impact

Let us briefly discuss the instantaneous post-clearing price impact during a continuous trading phase just after an auction. The following remarks are valid whenever there is a continuous trading phase right after the auction clearing (that is, after the open auction here). Let us consider the case of a trader sending a buy market order during the continuous trading phase just after auction clearing. This trader can expect to match up to all the remaining sell orders at p_a without impacting the price. Once the liquidity at p_a is consumed, sending an additional buy volume $q > 0$ will result in a sub-linear price impact. Indeed, since $\langle \tilde{\rho}_S \rangle$ has been observed to be linear around 0 (peak excluded), we may write $\langle \tilde{\rho}_S \rangle(x) = a_1 + b_1 x$ on this neighborhood so that we have on average

$$\int_0^x \langle \tilde{\rho}_S \rangle(u) du = q, \quad (8)$$

which implies

$$\frac{b_1}{2} x^2 + a_1 x - q = 0. \quad (9)$$

Hence, the post-clearing instantaneous price impact x is sub-linear and ranges between a square root limit when $q \gg \frac{a_1^2}{2b_1}$ and a linear impact limit $q \ll \frac{a_1^2}{2b_1}$. This reproduces in a stylized way the crossover between linear and square-root market impact observed in continuous double auctions (Bucci et al., 2019). The latter can be explained for example by assuming the existence of a hidden, latent LOB Tóth et al. (2011), which is only

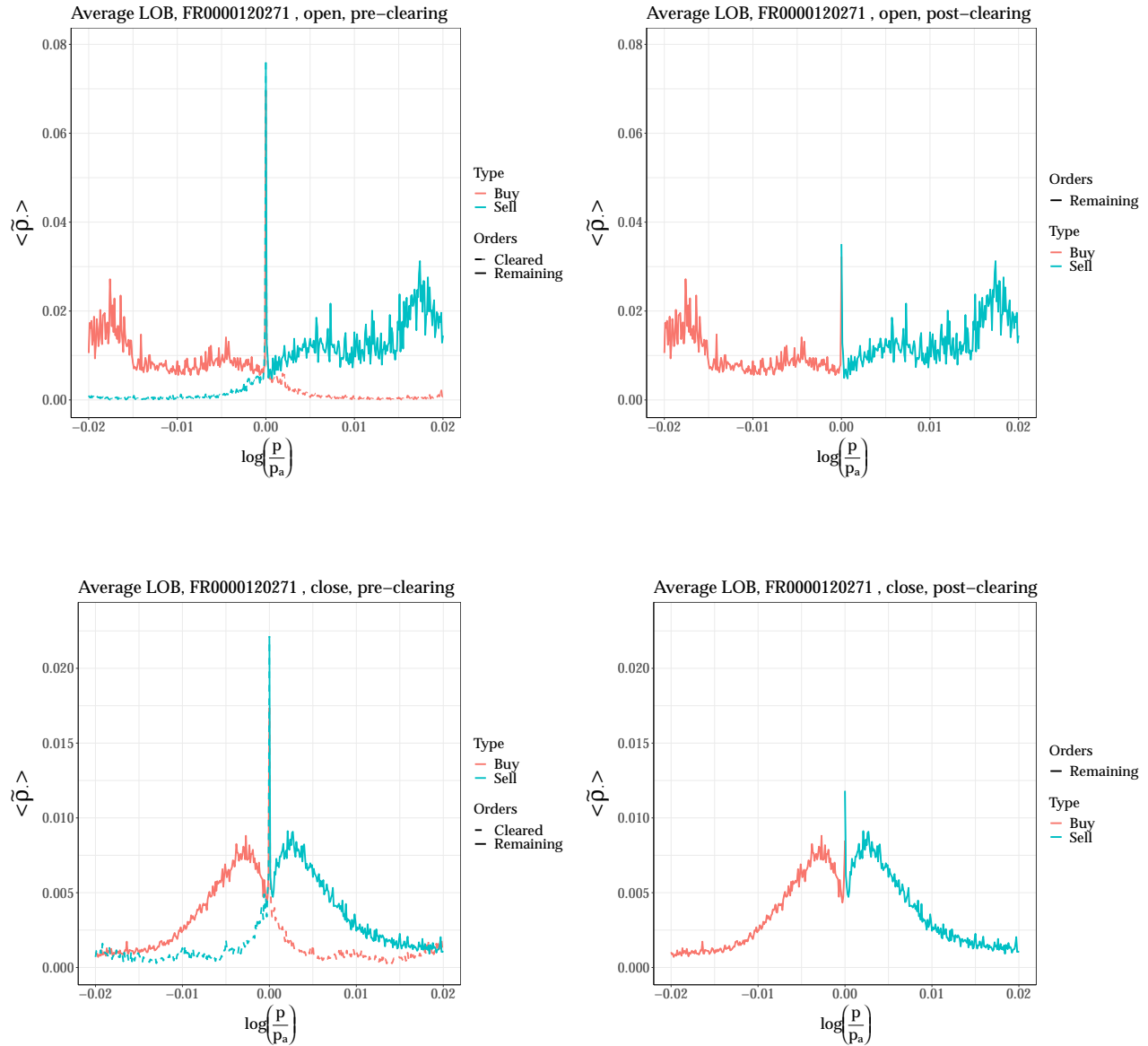


FIG. 2: Average density of the limit order book $\langle \tilde{\rho}_\bullet \rangle$ as a function of the log difference from the auction price p_a at the opening auction (top) and at the closing auction (bottom); left plots: pre-clearing, right plots: post-clearing (right). TTE.PA (TotalEnergies) between 2013 and 2017. In all panels, the mean density is computed on price intervals of size $\delta x = 1\text{bp}$ over $N = 1266$ days.

partially revealed but whose shape largely determines that of market impact. At auctions times instead, market participants are forced to reveal their intentions at least in the vicinity of p_a , and one can relate the auction LOB with the latent LOB.

C. Breakdown by market participant latency

Figure 3 displays a breakdown of the average empirical densities $\langle \tilde{\rho}_\bullet \rangle$ at the closing auctions by the speed of market participants. We used the latency flag in our data which specifies the HFT category of the order sender as per the AMF definition¹. Let us make three remarks regarding Figure 3. First, we notice that the MIX LOB has the same order of magnitude and shape as the total LOB (Fig. 2, bottom). This indicates that the contribution of traders flagged as fast (HFT) and slow (NON) to the liquidity provision of the closing auction (limit orders in the neighbourhood of the auction price) is smaller than the contribution of investment banks (flagged MIX). Second, the HFT LOB does not display an outstanding peak of volumes at the auction price. This suggests that this peak is actually caused by slow traders and may result in auction price pinning. Third, Figure 3 deals with the most liquid stock of the sample, but some stocks have a very small HFT-flagged LOB with the same order of magnitude as the low frequency LOB: HFT-flagged traders do not place sizeable limit orders in the closing auction of all stocks.

As stated in AMF (2017); Benzaquen and Bouchaud (2018), open markets are dominated by fast trading algorithms, which suggests considering the HFT LOB only (up to a multiplicative constant) when relating the auction LOB with the latent continuous-auction LOB. In this setting, the post-clearing price impact is much closer to a square root because of the sharp linear shape of the HFT LOB that vanishes around the current price.

D. Breakdown by account type

Figure 4 shows a breakdown of the average empirical densities $\langle \tilde{\rho}_\bullet \rangle$ at the closing auction by the account type. This particular flag tells on whose behalf an order was sent: client account, market maker, own account, parent company account, retail market organization (RMO), and retail liquidity provider (RLP). We notice that traders operating on behalf of their own account, which includes a significant fraction of investment banks' activities, and market makers provide most of the liquidity in the vicinity of the auction price. In addition, the density of orders sent on behalf of clients and slow traders have the same shape (see Fig. 3).

This decomposition will be valuable in designing realistic agent-based models (in addition to incorporating multi-time scale liquidity). We argue that the difference in size between market participants is hardly negligible for one to consider a continuum of heterogeneous independent agents².

¹ A participant is considered a high-frequency trader (HFT) if he meets one of the two following conditions:

- The average lifetime of its canceled orders is less than the average lifetime of all orders in the book, and it has canceled at least 100,000 orders during the year.
- The participant must have canceled at least 500,000 orders with a lifetime of fewer than 0.1 seconds, and the top percentile of the lifetime of its canceled orders must be less than 500 microseconds.

An investment bank meeting one of these conditions is described as mixed-HFT (MIX). If a participant does not meet any of the above conditions, it is a non-HFT (NON).

² In fact, there are only 126 authorized participants on the cash market (that includes equities) of Euronext Paris. See: <https://live.euronext.com/en/resources/members-list>.

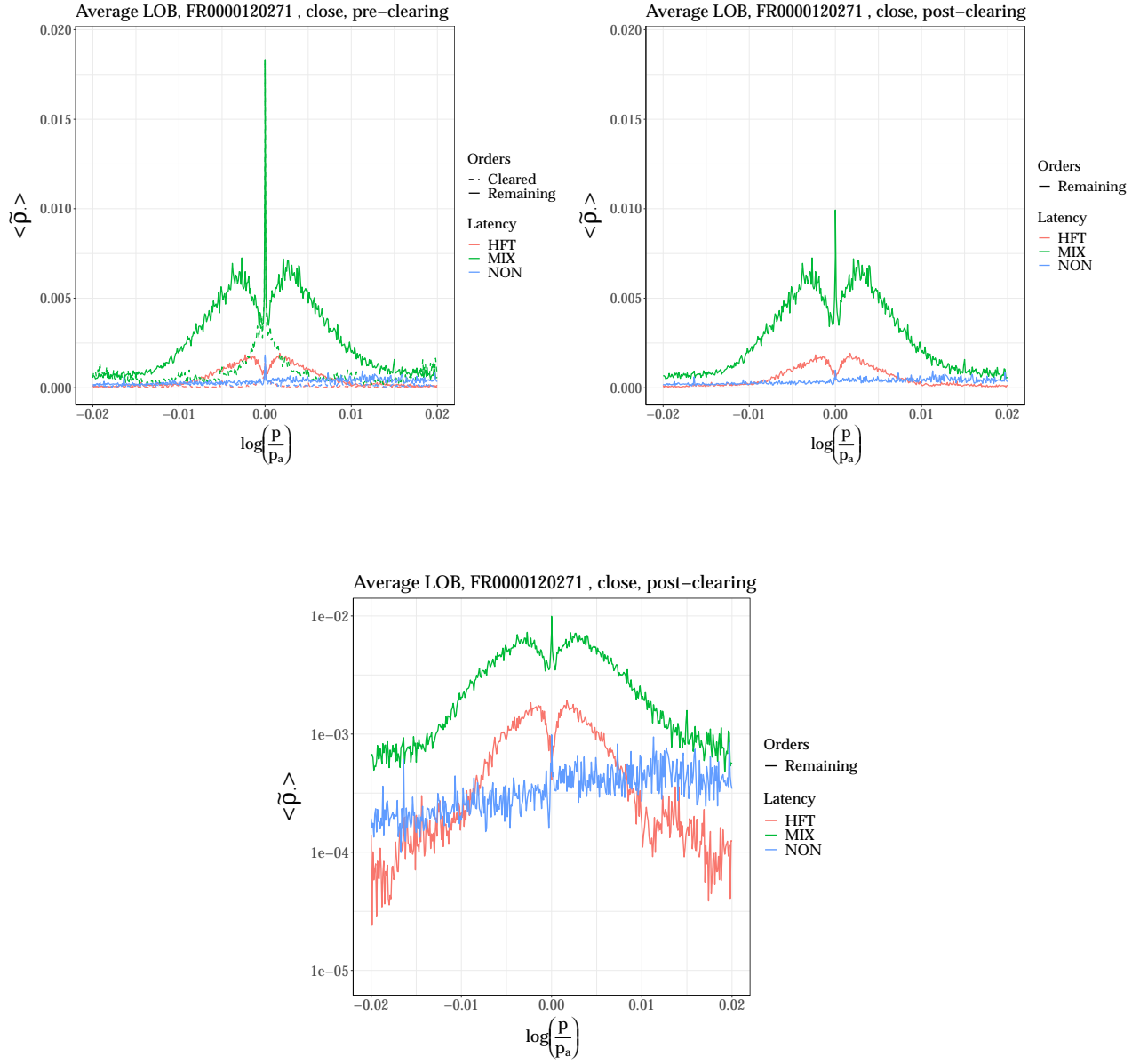


FIG. 3: Average density of the limit order book $\langle \tilde{\rho}_\bullet \rangle$ as a function of the log difference from the auction price p_a : breakdown by user latency of the average LOB during the closing auction just before the clearing (left), right after the clearing (right and bottom), with Y-axis in a log-scale (bottom) for TTE.PA between 2013 and 2017. The HFT flag denotes pure high frequency traders, MIX denotes investment banks with high frequency trading activities, and NON denotes traders without HFT activities.

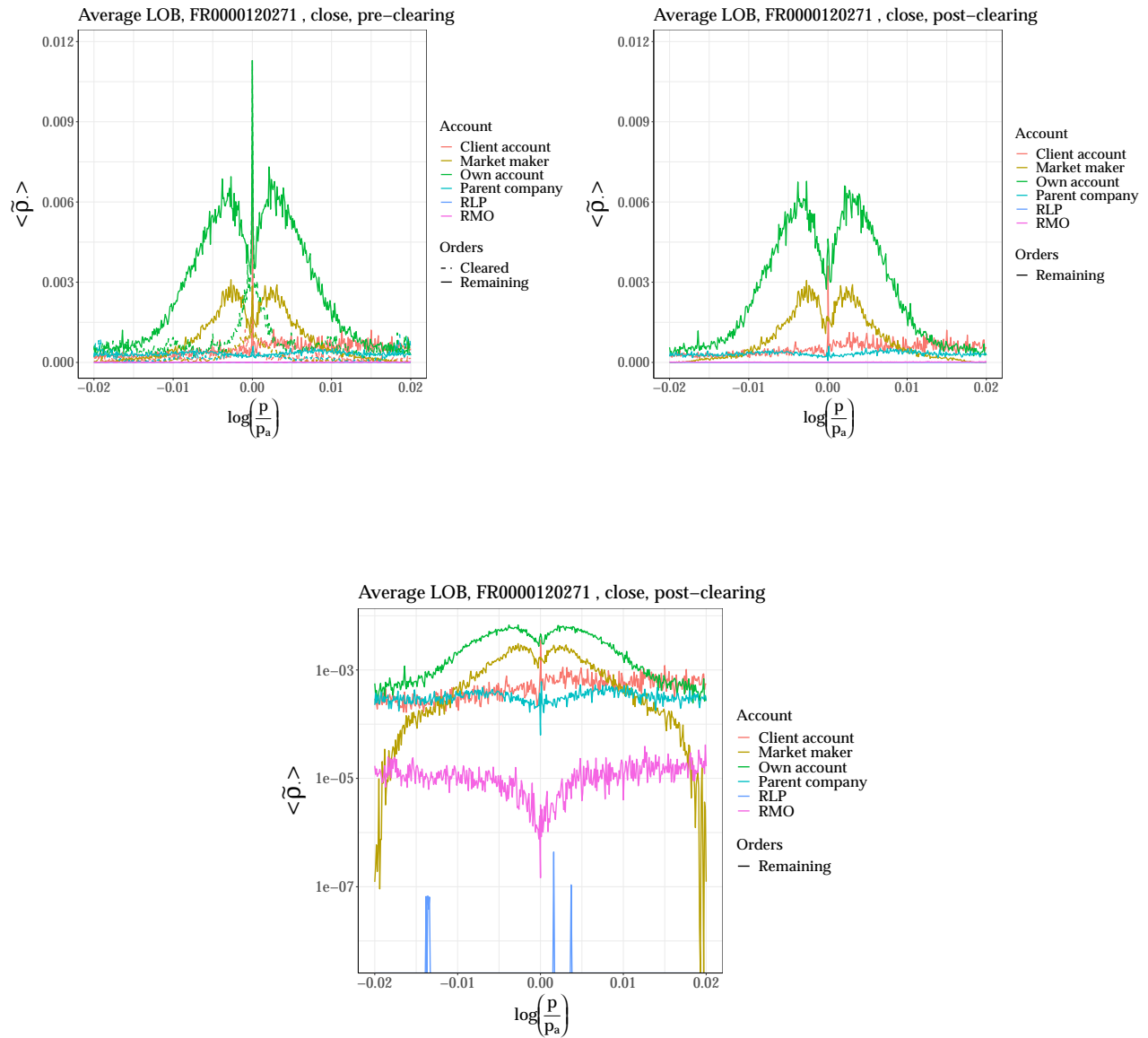


FIG. 4: Average density of the limit order book $\langle \tilde{\rho}_\bullet \rangle$ as a function of the log difference from the auction price p_a : breakdown of the average LOB during the closing auction by user account type just before the clearing (left), right after the clearing (right and bottom), with Y-axis in a log-scale (bottom) for TTE.PA between 2013 and 2017. Colors represent orders executed on the behalf of: a client account, a market maker, an own account, a parent company account, a retail market organization (RMO), and a retail liquidity provider (RLP).

V. PRICE IMPACT

This section investigates a set of statistical regularities of the static price impact in equity auctions. First, for $t = T_a$, we highlight the existence of a significant zero impact volume below which the auction price would not have changed. Removing this zero-impact part, we show that the auction price impact can be considered linear, not only on average but for most days. We also derive a simple formula for the impact slope that we validate empirically using a simplified optimization routine. Then, we briefly examine the influence of derivatives' expiry days on closing auctions. Finally, we explore the auction impact kinematics throughout the accumulation period.

A. Zero impact: $\omega < \omega_{\bullet}^{(0)}$

When inspecting the price impact function over several days and auctions, we observe that the minimal volume necessary to change the auction price ($Q_a \times \omega_{\bullet}^{(0)}$ using the notations of Proposition 3), can be much larger than the typical volumes needed to impact the price further ($Q_a \times \delta\omega_{\bullet}^{(i)}$, $i \geq 1$). A compelling example is given by Figure 5, which shows the price impact function for TTE.PA at the closing auction of May 5, 2017, with the following quantities: $p_a = 48.00\text{€}$, $Q_a = 2,246,617$, $\omega_B^{(0)} = 27.45\%$, and $\omega_S^{(0)} = 9.61\%$. Hence, if sent just before T_a , a buy order of a cash volume lower than $Q_a \times \omega_B^{(0)} \times p_a = 29.6$ million€ would not have resulted in an auction price change. Similarly a sell order of a cash volume lower than $Q_a \times \omega_S^{(0)} \times p_a = 10.3$ million€ would have had zero impact.

In our sample, zero price impact is present in more than 98% of the total processed days and sides. This means that in more than 98% of the time, sending one share, either on the buy or the sell side, will not change the

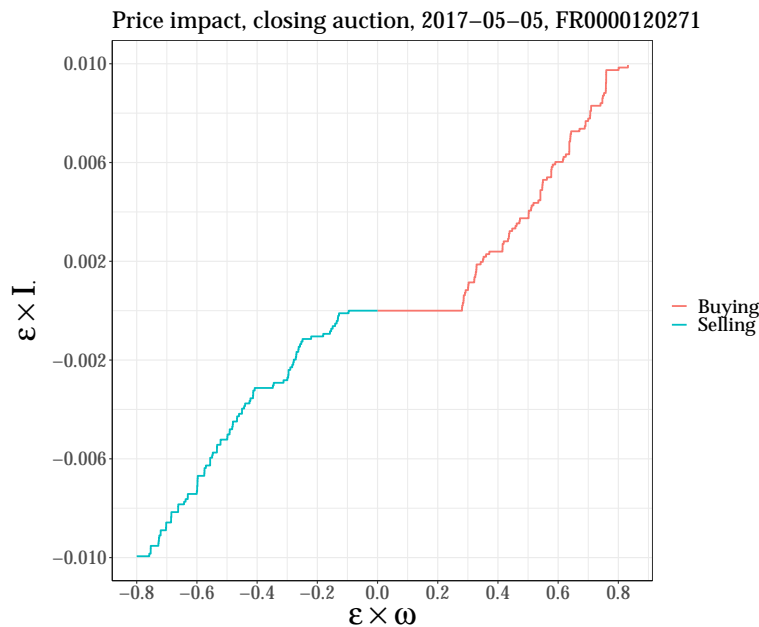


FIG. 5: Virtual price impact $\varepsilon \cdot I$ as a function of the (scaled) added signed volume $\varepsilon \cdot \omega$ at the closing auction of TTE.PA on 2017-05-05. $\varepsilon = +1$ for a buy market order and $\varepsilon = -1$ for sell market order.

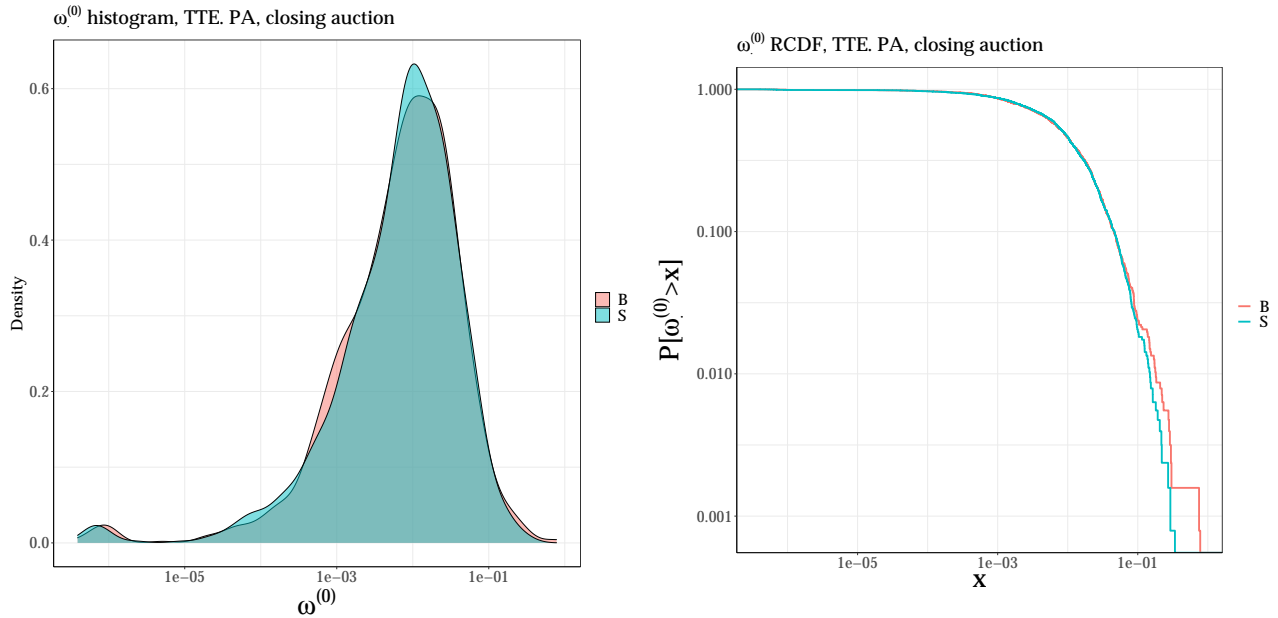


FIG. 6: Left panel: smoothed histograms of zero impact volumes (buy and sell) $\omega_{\bullet}^{(0)}$; right panel: empirical reverse cumulative distribution function (RCDF) of zero impact volumes $\omega_{\bullet}^{(0)}$.

auction price. In addition, and maybe more surprisingly, zero impact on both sides simultaneously is by far the most common situation.

This comes from the fact that the prices are discrete and thus the cumulative buy and sell volumes $D(p)$ and $S(p)$ are step functions. At the auction price, these steps only overlap partially. To change the auction price, one needs to shift vertically either D or S in such a way that the overlap at the auction price disappears (see Figure 1 for an illustration). Thus, zero price impact only disappears when both $V_B(p_a)$ and $V_S(p_a)$ only have one share at most at p_a . Price impact can be zero for relatively large orders because of the peak of volume at p_a : recall that the (scaled) zero-impact volume $\omega_{\bullet}^{(0)}$ is the minimal volume needed to change the auction price; by the definition of $\omega_{\bullet}^{(0)}$ in Proposition 3, having large matched buy and sell volumes at the auction price leads to large zero impact volumes on both sides (see Figure 1). This is confirmed empirically: we report in Table II the probability $\mathbb{P}_{1\%}$ to send a market order of size $q = 1\% \times Q_a$ just before the clearing without moving the closing price. For the stocks in our sample, this probability ranges from 46% to 74%. Since September 28, 2015, a 30-second random time window was introduced in Euronext Paris auctions. Thus, the closing auction clearing can happen anytime between 17:35:00 and 17:35:30 (and between 09:00:00 and 09:00:30 for the opening auction). This prevents fast agents from using their low latency to size their trades so as to have zero impact.

We also report several statistical observations on $\omega_B^{(0)}$ and $\omega_S^{(0)}$. First, their statistical distribution can not be distinguished (as shown in Figure 6). This is confirmed by a Kolmogorov-Smirnov test reported in Table II, which also reports the empirical Spearman correlation between these two quantities: quite surprisingly, given the observation above, the correlation between $\omega_B^{(0)}$ and $\omega_S^{(0)}$ is rather weak, -0.15 on average, and is non-significant for some very liquid stocks (e.g., TTE.PA the most traded stock in our dataset). This confirms that zero-impact is mostly a mechanical effect, not a strategic one.

Let us finally compare $\delta\omega_{\bullet}^{(0)} = \omega_{\bullet}^{(0)}$, the minimal scaled volume needed to move the auction price, to $\delta\omega_{\bullet}^{(i)} = \omega_{\bullet}^{(i)} - \omega_{\bullet}^{(i-1)}$, $i \geq 1$, the minimal scaled volumes needed to take the price from $p_{\bullet}^{(i)}$ to $p_{\bullet}^{(i+1)}$ (see Proposition 3). Table III presents results for the stock TTE.PA of pairwise Kolmogorov-Smirnov tests on the empirical distribution functions of $\delta\omega_{\bullet}^{(i)}$ and $\delta\omega_{\bullet}^{(j)}$. For the sake of brevity, results are presented for $i, j \leq 10$, but the statistical testing has actually been conducted up to $i, j = 40$. We clearly observe that $\delta\omega_{\bullet}^{(0)}$ and $\delta\omega_{\bullet}^{(1)}$ have

TABLE II: Spearman correlation and Kolmogorov-Smirnov test statistics for $\omega_B^{(0)}$ and $\omega_S^{(0)}$, as well as the probability $\mathbb{P}_{1\%}$ to send a market order of size $q = 1\% \times Q_a$ without impacting the auction price just before the clearing across the stocks in our sample.

ISIN	$\text{cor}(\omega_B^{(0)}, \omega_S^{(0)})$	KS statistic($\omega_B^{(0)}, \omega_S^{(0)}$)	$\mathbb{P}_{1\%}$	Observations
CH0012214059	-0.559***	0.088*	64%	510
FR0000031122	-0.267***	0.056	67%	1009
FR0000045072	-0.321***	0.035	65%	1014
FR0000073272	-0.102**	0.049	66%	1015
FR0000120073	-0.210***	0.025	64%	1014
FR0000120172	-0.156***	0.045	66%	1268
FR0000120271	-0.048	0.022	46%	1266
FR0000120354	-0.152***	0.088***	70%	1014
FR0000120404	-0.089**	0.052	69%	1015
FR0000120537	-0.004	0.044	70%	504
FR0000120578	-0.139***	0.054*	48%	1268
FR0000120628	-0.263***	0.043	64%	1261
FR0000120644	-0.166***	0.027	60%	1012
FR0000120685	-0.209***	0.044	68%	1014
FR0000121014	-0.272***	0.021	68%	1014
FR0000121147	-0.015	0.027	73%	1013
FR0000121261	-0.225***	0.027	65%	1013
FR0000121501	-0.311***	0.053	68%	1014
FR0000121667	-0.338***	0.021	69%	1012
FR0000121972	-0.095***	0.035	58%	1264
FR0000124141	-0.288***	0.026	73%	1012
FR0000125007	-0.14***	0.036	57%	1265
FR0000125338	-0.172***	0.042	68%	1012
FR0000125486	-0.132***	0.038	59%	1013
FR0000127771	-0.248***	0.04	68%	1015
FR0000130338	-0.098*	0.033	74%	613
FR0000130809	-0.061*	0.032	56%	1259
FR0000131104	-0.128***	0.049	53%	1264
FR0000131708	-0.118**	0.042	68%	771
FR0000131906	-0.075**	0.032	62%	1269
FR0000133308	-0.242***	0.043	67%	1012
FR0010208488	-0.271***	0.025	68%	1010
FR0013176526	-0.349***	0.065	57%	401
NL0000235190	-0.096***	0.035	61%	1264

The symbols ***, **, and * indicate significance at the 0.1%, 1%, and 5% level, respectively.

specific statistical properties, while the distributions of the incremental volumes $\delta\omega_{\bullet}^{(i)}$ for $2 \leq i \leq 32$ could hardly be distinguished as the null hypothesis could not be rejected at the 1% significance level. Figure 7 shows smoothed histograms and empirical reverse cumulative distribution function for $\delta\omega_{\bullet}^{(i)}$, $0 \leq i \leq 5$. This observation is not easily generalized to all stocks since additional factors come into play: small tick vs large tick stocks as well as the introduction of the 30-second random clearing window in September 2015: these factors have a non-negligible influence on the distribution of $\delta\omega_{\bullet}^{(i)}$ s across different stocks over the years.

B. Linear impact: $\omega_{\bullet}^{(0)} < \omega < \omega_{\bullet}^{(\max)}$

According to (Donier and Bouchaud, 2016), in a Walrasian auction with continuous prices, average volumes around the auction price are non-null, which leads to a linear impact (in a first-order expansion), while in a continuous double auction, average volumes vanish around the current price and lead to a square root impact.

TABLE III: Kolmogorov-Smirnov statistics for pairs of rescaled incremental volumes $\delta\omega_{\bullet}^{(i)}$ and $\delta\omega_{\bullet}^{(j)}$ for the stock TTE.PA.

	$\delta\omega^{(0)}$	$\delta\omega^{(1)}$	$\delta\omega^{(2)}$	$\delta\omega^{(3)}$	$\delta\omega^{(4)}$	$\delta\omega^{(5)}$	$\delta\omega^{(6)}$	$\delta\omega^{(7)}$	$\delta\omega^{(8)}$	$\delta\omega^{(9)}$	$\delta\omega^{(10)}$
$\delta\omega^{(0)}$											
$\delta\omega^{(1)}$	0.091***										
$\delta\omega^{(2)}$	0.047**	0.08***									
$\delta\omega^{(3)}$	0.063***	0.103***	0.034								
$\delta\omega^{(4)}$	0.057***	0.105***	0.033	0.023							
$\delta\omega^{(5)}$	0.053**	0.089***	0.02	0.026	0.028						
$\delta\omega^{(6)}$	0.055**	0.112***	0.04*	0.021	0.028	0.032					
$\delta\omega^{(7)}$	0.068***	0.117***	0.044*	0.019	0.026	0.031	0.024				
$\delta\omega^{(8)}$	0.043*	0.086***	0.02	0.03	0.03	0.018	0.037	0.037			
$\delta\omega^{(9)}$	0.047**	0.091***	0.019	0.025	0.021	0.02	0.032	0.036	0.016		
$\delta\omega^{(10)}$	0.042*	0.081***	0.022	0.04*	0.037	0.022	0.043*	0.041*	0.016	0.023	

The symbols ***, **, and * indicate significance at the 0.1%, 1%, and 5% level, respectively.

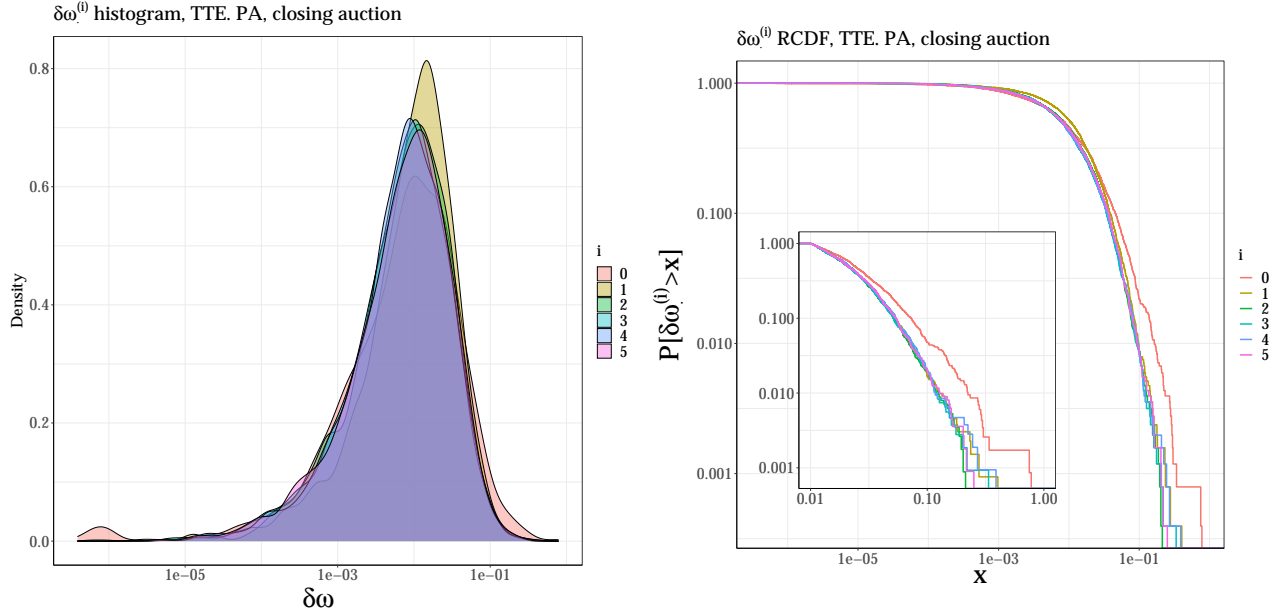


FIG. 7: Left panel: smoothed histograms of scaled incremental volumes $\delta\omega_{\bullet}^{(i)}$ for $i = 0 \dots 5$; right panel: empirical reverse cumulative distribution function (RCDF) of scaled incremental volumes $\delta\omega_{\bullet}^{(i)}$ for $i = 0 \dots 5$.

It is useful to first assume that price is continuous in order to derive a simple condition the price impact to be strictly linear. If we send a buy market order of size $\omega \times Q_a$ before the auction clearing, and assuming we work in a log-price frame of reference $x = \log(p/p_a)$ in a continuous price setting, we have

$$\begin{cases} S(0) = D(0), \\ S(I_B(\omega)) = D(I_B(\omega)) + \omega Q_a, \end{cases} \quad (10)$$

hence,

$$S(I_B(\omega)) - S(0) = D(I_B(\omega)) - D(0) + \omega Q_a. \quad (11)$$

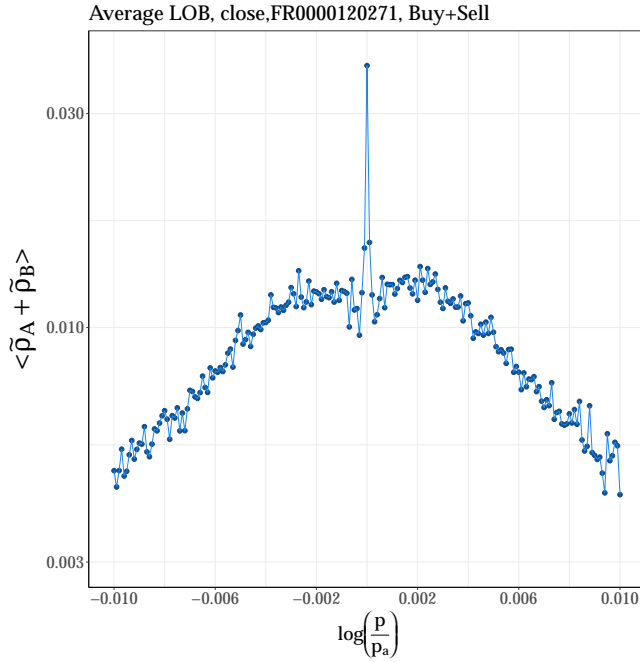


FIG. 8: Average empirical density of total (buy + sell) volumes for TTE.PA at the closing auction.

Donier and Bouchaud (2016) perform a first-order expansion to write

$$\partial_x S(0) \times (I_B(\omega) - 0) = \partial_x D(0)(I_B(\omega) - 0) + \omega Q_a, \quad (12)$$

and approximate

$$I_B(\omega) = \frac{1}{\tilde{\rho}_S(0) + \tilde{\rho}_B(0)} \times \omega. \quad (13)$$

However, instead, we use equation (11) to find exactly

$$\int_0^{I_B(\omega)} (\tilde{\rho}_S + \tilde{\rho}_B)(x) dx = \omega, \quad (14)$$

thus

$$\begin{aligned} I_B(\omega) &= F^{-1}(\omega), \\ F(x) &= \int_0^x (\tilde{\rho}_S + \tilde{\rho}_B)(u) du. \end{aligned} \quad (15)$$

Having a linear impact requires that F^{-1} and F are linear functions, therefore that $x \mapsto (\tilde{\rho}_S + \tilde{\rho}_B)(x)$ is constant.

Figure 8 shows the average empirical density $\langle \tilde{\rho}_S + \tilde{\rho}_B \rangle_d$ of the sum of buy and sell volumes for the most liquid stock in the sample. It strongly suggests the existence of a price interval, on each side of the auction price, in which the sum of buy and sell volumes can be well approximated by a constant.

We now include this observation in the discrete-price theoretical framework introduced Section II and we prove in Proposition 4 that if buy and sell densities sum up to a constant around the auction price p_a (removing the zero-impact part), price impact is linear.

Proposition 4. If $x \mapsto (\tilde{\rho}_S + \tilde{\rho}_B)(x)$ is constant on some intervals $] - \Delta_S, 0[$ and $]0, \Delta_B[$, then the price impact I_\bullet is linear. More precisely, if $\tilde{\rho}_S(x) + \tilde{\rho}_B(x) = \widetilde{\mathcal{L}}_B$ positive constant for all $x \in]0, \Delta_B[$ and $\tilde{\rho}_S(x) + \tilde{\rho}_B(x) = \widetilde{\mathcal{L}}_S$ positive constant for all $x \in] - \Delta_S, 0[$, then for all i such that $I(\omega^{(i)}) < \Delta$, we have

$$I(\omega^{(i)}) - I(\omega^{(0)}) = \frac{1}{p^{(1)} \widetilde{\mathcal{L}}} \left(\omega^{(i)} - \omega^{(0)} \right), \quad (16)$$

where we omitted the $\bullet \in \{B, S\}$ notation from I , ω , $p^{(1)}$ and $\widetilde{\mathcal{L}}$. Recall that $p_\bullet^{(1)}$ is the first non empty price tick after (resp. before) the auction price when $\bullet = B$ (resp. when $\bullet = S$), as in Proposition 3.

The proof of Proposition 4 is given in Appendix B. Notice that $\widetilde{\mathcal{L}}$ represents a constant scaled liquidity around p_a . Also, since $\widetilde{\mathcal{L}}$ and ω are both scaled by Q_a , the price impact as written in the right-hand side of equation (16) does not depend on the auction volume Q_a . For large-tick stocks, if $V_B(p) + V_S(p) = V_c$ constant around p_a , then the scaled liquidity is given by $\widetilde{\mathcal{L}} = V_c / (Q_a \theta)$, where θ is the tick size. For small-tick stocks, one can obtain an approximation by substituting θ with a fraction of the average spread.

Following Proposition 4, we want to characterize the intervals in which $\tilde{\rho}_S + \tilde{\rho}_B$ can be considered constant. Therefore we need to find $\widetilde{\mathcal{L}}_\bullet$ and Δ_\bullet for $\bullet \in \{B, S\}$, such that:

$$\begin{aligned} \tilde{\rho}_S(x) + \tilde{\rho}_B(x) &= \widetilde{\mathcal{L}}_B \text{ for all } x \in]0, \Delta_B[; \\ \tilde{\rho}_S(x) + \tilde{\rho}_B(x) &= \widetilde{\mathcal{L}}_S \text{ for all } x \in] - \Delta_S, 0[. \end{aligned} \quad (17)$$

For symmetry reasons, we focus on Δ_B and $\widetilde{\mathcal{L}}_B$: the problem is to find Δ_B and $\widetilde{\mathcal{L}}_B$ for a given day d by resorting to a simple change point detection algorithm. This method minimizes the residual sum of squared errors between $\log(\tilde{\rho}_S(x) + \tilde{\rho}_B(x))$ and its mean $\eta(y)$ for $x \in]0, y]$ plus the residual sum of errors of a linear fit of $\log(\tilde{\rho}_S(x) + \tilde{\rho}_B(x))$ for $x > y$. We choose to work with logarithms, since errors are multiplicative. The resulting cost function is:

$$\begin{aligned} f(y) &= \sum_{0 < x \leq y} |\log(\tilde{\rho}_S(x) + \tilde{\rho}_B(x)) - \eta(y)|^2 + \sum_{x > y} \left| \log(\tilde{\rho}_S(x) + \tilde{\rho}_B(x)) - \hat{\beta}(y)x - \hat{\alpha}(y) \right|^2; \\ \eta(y) &= \frac{1}{N_y} \sum_{0 < x \leq y} \log(\tilde{\rho}_S(x) + \tilde{\rho}_B(x)), \end{aligned} \quad (18)$$

where $(\hat{\alpha}(y), \hat{\beta}(y))$ is the linear regression estimate of $\log(\tilde{\rho}_S(x) + \tilde{\rho}_B(x))$ over x for $x > y$, and N_y is the number of non-null observations $(x, \log(\tilde{\rho}_S(x) + \tilde{\rho}_B(x)))$ for $x \in]0, y]$. We then define:

$$\Delta_B = \arg \min_y f(y). \quad (19)$$

This definition means that for $x \leq \Delta_B$, the sum of the logarithm of the sum of scaled empirical buy and sell densities is better approximated by its mean than by a non-constant (linear) fit, whereas for $x > \Delta_B$, the opposite holds. Then, we calculate $\widetilde{\mathcal{L}}_B$ as the mean of $(\tilde{\rho}_S + \tilde{\rho}_B)(x)$ for $0 < x \leq \Delta_B$ in order to avoid an underestimation due to the convexity of the exponential function. Finally, we define $\omega_\bullet^{(\max)}$ as the maximum scaled volume of a market order that would result in a null or linear impact, i.e.,

$$\omega_\bullet^{(\max)} = \omega_\bullet^{(0)} + \sum_{0 < |x| \leq \Delta_\bullet} \frac{V_B(x) + V_S(x)}{Q_a}. \quad (20)$$

Figure 9 shows examples for Δ detection using the previous optimisation for two different days at the closing auction, and plots in each case the theoretical impact given by Proposition 4 with respect to the actually observed impact function. One sees that the estimated cut-off Δ , as well as the slope estimate $(p^{(1)} \widetilde{\mathcal{L}})^{-1} \approx (p_a \widetilde{\mathcal{L}})^{-1}$, fit very well the actual slope and domain of the linear price impact. This is actually the case of most days, as shown by Figure 10, where we plot the observed slope against the theoretical slope.

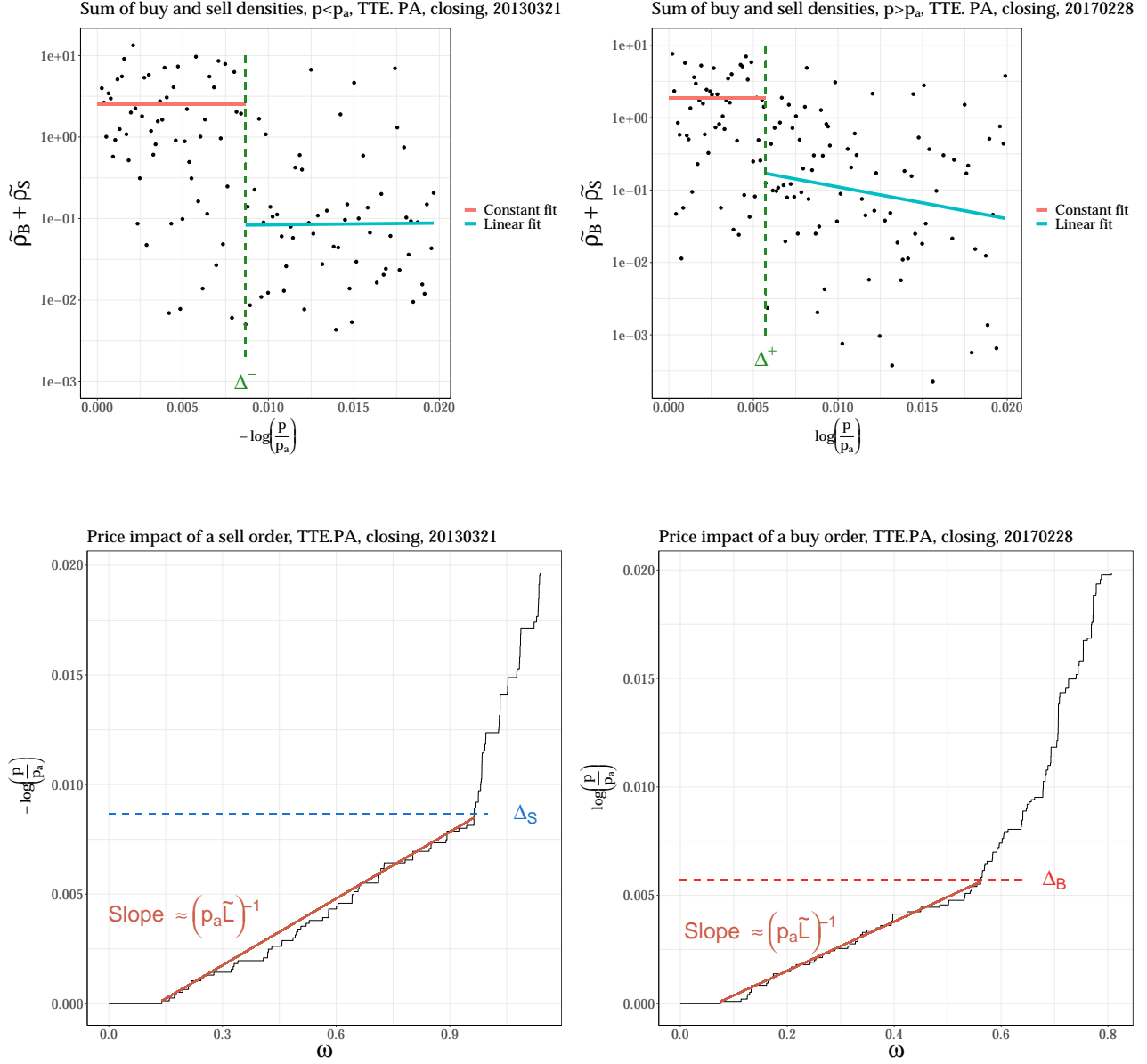


FIG. 9: Simplified changed point detection algorithm applied on the buy side of the closing auction of TTE.PA at 2013-03-21 (left) and the sell side of the closing auction of TTE.PA at 2017-02-28 (right). The upper plots show the sum of the buy and sell empirical densities and estimated cut-off Δ with a green dashed line. Lower plots show the fit of the estimated impact slope $(p^{(1)} \tilde{\mathcal{L}})^{-1} \approx (p_a \tilde{\mathcal{L}})^{-1}$ on the corresponding impact functions.

We also plot the smoothed histograms of Δ and $\omega^{(\max)}$ issued by our detection algorithm for the stock TTE.PA between 2013 and 2017 (1266 stock-days and two sides (buy and sell)) (see Fig. 11). Note that we truncated the closing auction snapshots at a maximum log-price distance $x \leq 2\%$, which is twice the average impact of a market order of a size equal to the auction volume Q_a . In addition, only fits with a number of points ≥ 20 are kept, which happens in about $\approx 90\%$ of the days and sides: this shows that the price impact is linear for most of the days with an average value of Δ above 50 basis points. Finally, $\mathbb{P}[\omega^{(\max)} > 0.5] = 0.73$: this means that

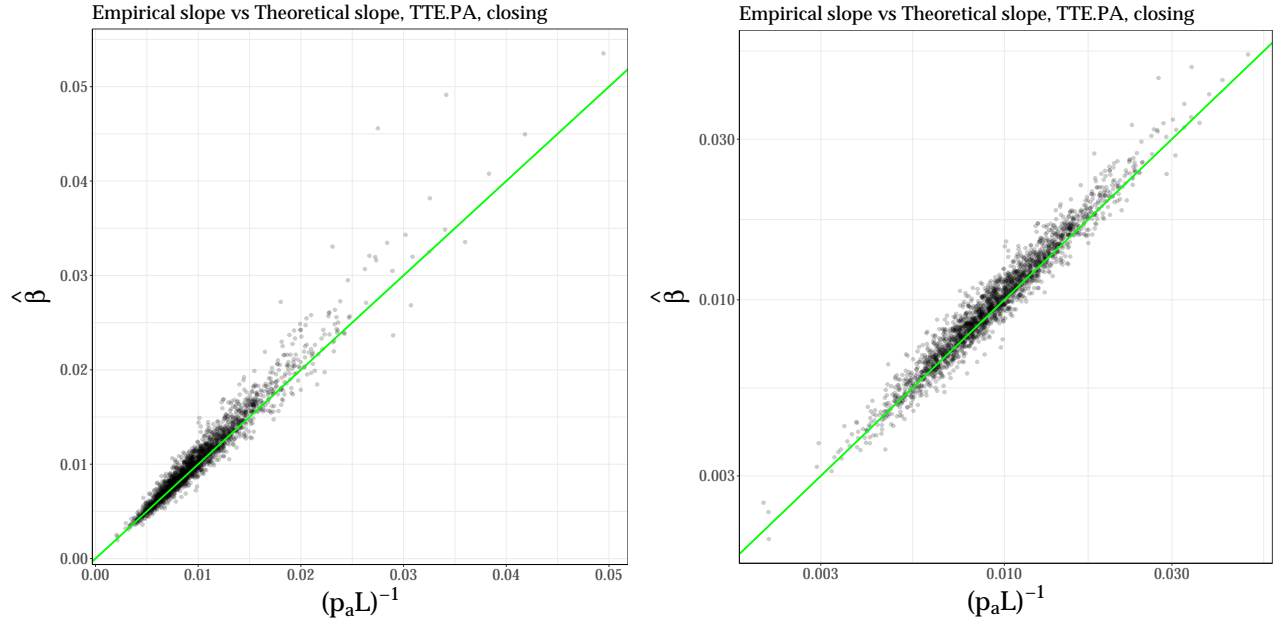


FIG. 10: Empirical slope $\hat{\beta}$ vs Theoretical slope $(p^{(1)} \tilde{\mathcal{L}})^{-1} \approx (p_a \tilde{\mathcal{L}})^{-1}$ given by equation (16) at the closing auction for TTE.PA. Left panel: normal scale. Right panel: log-log scale. A straight line with unit slope and null intercept is plotted in green for visual guidance.

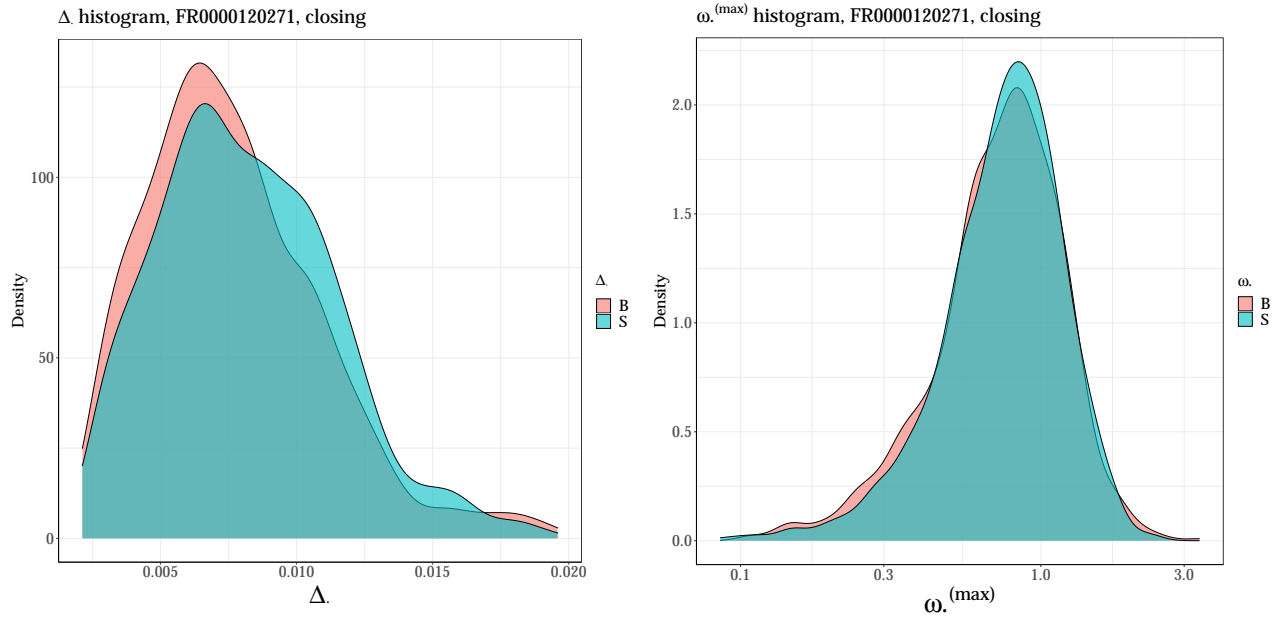


FIG. 11: Smoothed histograms of the maximum log-distance Δ over which the sum of the buy and sell densities can be considered constant (left) and the maximum scaled volume $\omega^{(\max)}$ that results in a null or linear impact. These are outputs of the optimisation of equation (18) applied on the closing auction of TTE.PA between 2013 and 2017.

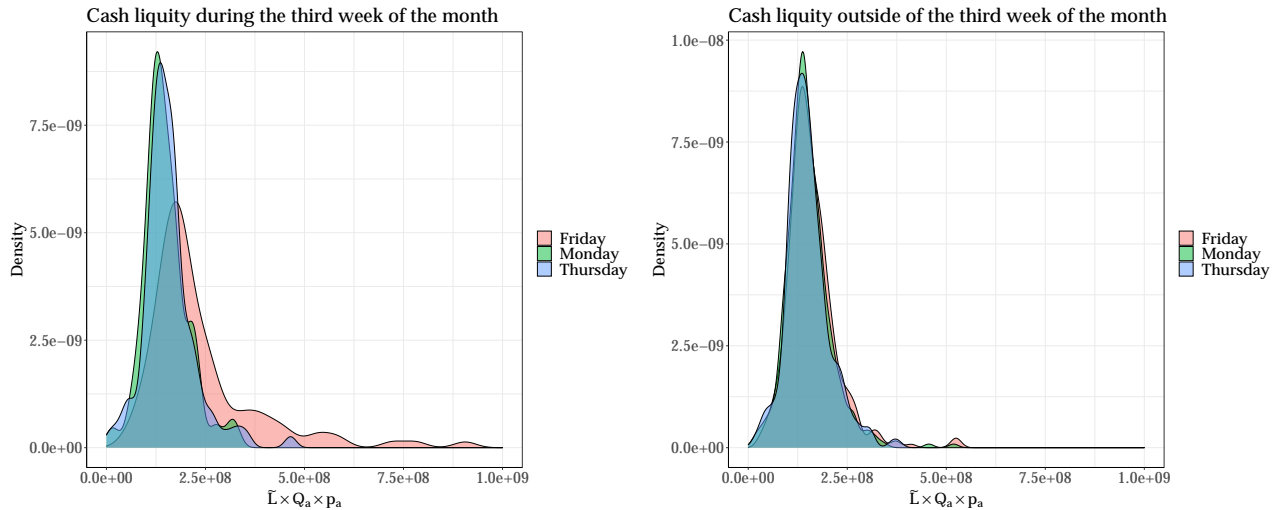


FIG. 12: Smoothed histograms of the closing auction estimated cash liquidity $L^{\$} := \tilde{\mathcal{L}} \times Q_a \times p_a$ during the third week of the month (left) and outside of the third week of the month (right).

a trader has 73% chance to execute 50% of the total auction volume just before the close clearing and still result in zero or linear impact.

C. Influence of derivatives expiry dates on the closing auction

When there is no derivatives expiry, cash liquidity defined by $L^{\$} := p_a \times Q_a \times \tilde{\mathcal{L}}$ whether on Friday or other days of the week (Fig. 12, right panel) seem to be drawn from the same distribution, as we could not reject the null hypothesis associated with Kolmogorov-Smirnov tests on cash liquidity for any pairs of weekdays outside the third week of the month. However, on expiry days (third Fridays of the month), cash liquidity is typically larger than for other weekdays during the same week and seem to be drawn from a different shifted distribution to the right (Fig. 12, left panel). This finding is confirmed by one tailed Kolmogorov-Smirnov tests on cash liquidity for Friday and any other weekday during the third weeks of a month. Therefore, the impact slope is typically smaller during expiry days and the final auction order book is more resistant to price changes.

D. Price impact kinematics

Lastly, we investigate how the virtual price impact behaves throughout the accumulation period. We construct successive snapshots at 5-second intervals for TTE.PA at the closing auction. Then, we compute the price impact for $t \leq T_a$ with $p_a \leftarrow p_t^{\text{ind}}$ and $Q_a \leftarrow Q_t^{\text{ind}}$. We define the absolute liquidity \mathcal{L}_t as the (constant) sum of buy and sell empirical densities at time t: $\mathcal{L}_t = (V_B + V_S)(t)/\delta p$ (Recall that the buy and sell densities sum up to a constant around the current indicative price). Similarly, we define $Q_t^{(\text{max})}$ as the maximum (absolute) volume that results in a null or linear impact time t. Figure 13 shows that averages of both the absolute liquidity (w.r.t. to Q_a) \mathcal{L}_t/Q_a and the fraction of the final liquidity $\mathcal{L}_t/\mathcal{L}_{T_a}$ follow the same pattern, i.e., a strong concave monotonicity at the start of the accumulation period followed by strong convex evolution as the clearing nears. Likewise, the average of the maximum linear volume with respect to the final volume $Q_t^{(\text{max})}/Q_a$ has the same

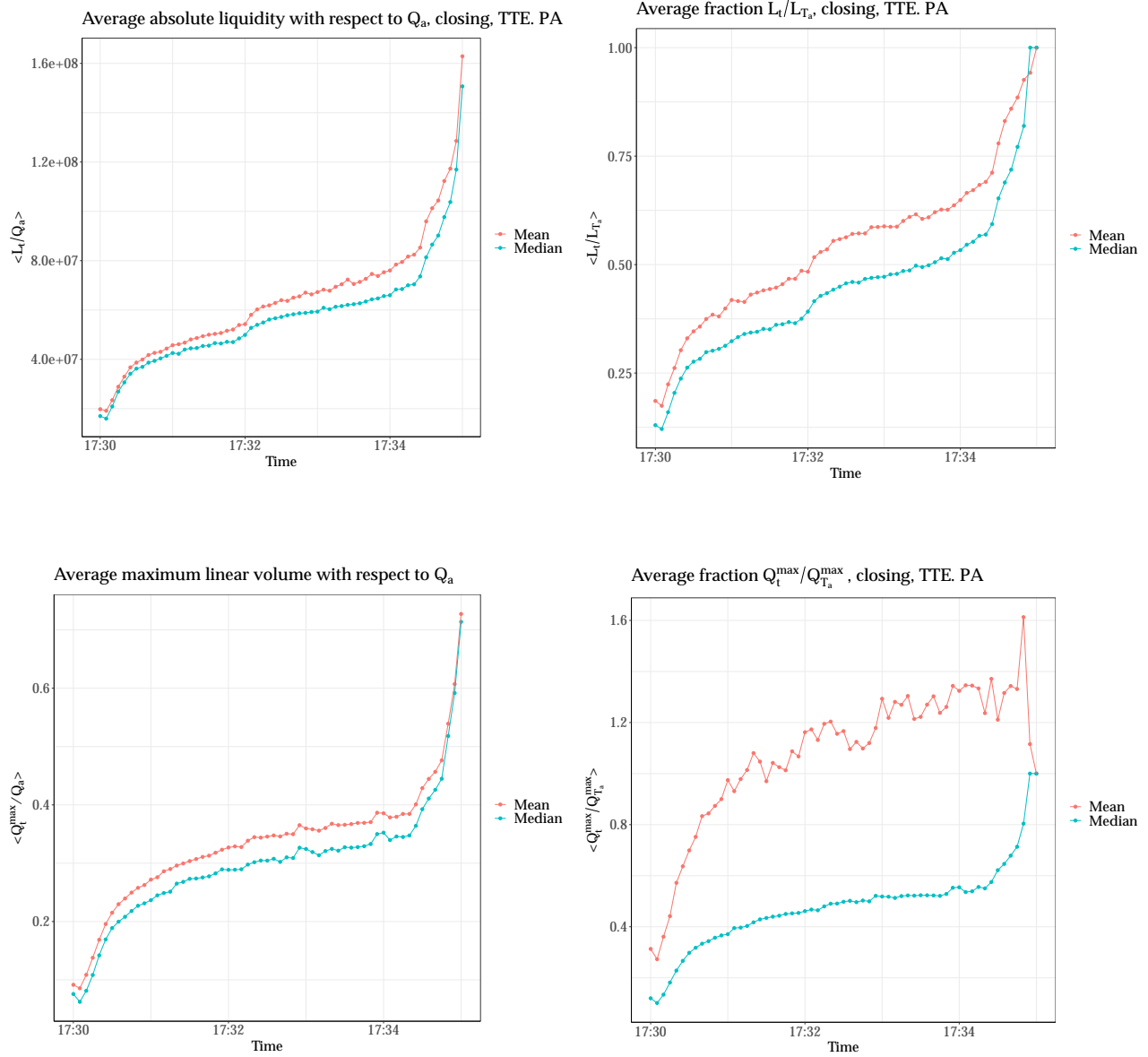


FIG. 13: Average absolute liquidity with respect to Q_a during the closing auction (upper left). Average fraction $\langle L_t/L_{T_a} \rangle$ of the absolute liquidity at time t L_t by final-at the clearing- liquidity L_{T_a} (upper right). Average (absolute) maximum linear-impact volume with respect to Q_a during the closing auction $\langle Q_t^{(max)}/Q_a \rangle$ (lower left). Average fraction $\langle Q_t^{(max)}/Q_{T_a}^{(max)} \rangle$ of the absolute maximum linear-impact volume at time t $Q_t^{(max)}$ by final -at the clearing- absolute maximum volume $Q_{T_a}^{(max)}$ (lower right).

shape. Nonetheless, the average mean of $Q_t^{(\max)}/Q_{T_a}^{(\max)}$ has a more complex pattern and suggests a strong effect of cancellations.

VI. CONCLUSION

The discrete nature of prices in limit order books mechanically causes the price impact at auction time to be zero at first, sometimes for quite a substantial fraction of the total exchanged volume. Surprisingly, zero price impact happens most of the time simultaneously on both sides of the auction book, for additional sell and buy market orders or equivalently for cancellations of buy or sell market orders. For volumes larger than zero-impact ones, price impact at auction time is linear in a limited price range around the auction price not only on average but for more than 90% of days. The theoretical work of Donier and Bouchaud (2016) shows the linearity of the auction impact locally around the auction price using a first-order expansion and under strong regularity assumptions of supply and demand in a continuous price setting. Here, we showed that the linearity of auction impact is due instead to the fact that the sum of buy and sell volumes around the auction price is constant.

While this work mainly describes the final result of the order accumulation process and characterizes the limit order book at the auction time, a more microscopic description of the dynamics of order submission, cancellation, and perhaps diffusion (price update) is needed. Even though market orders submitted during the accumulation period do not play a significant role in shaping the price response of the final limit order book, the action-reaction game between market orders and limit orders throughout the auction (Besson and Fernandez, 2021; Raillon, 2020) is probably a major driver of its dynamics. Similarly, the interplay between the various categories of agents (HFTs, market makers, agents trading on their behalf, or agents trading on behalf of their clients, . . .) is clearly of great interest. For example, Boussetta et al. (2017) show that HFTs submit their orders in a markedly different way than slow traders. A good starting point would be a substantial modification of the model of Donier and Bouchaud (2016) in the spirit of the work done by Lemhadri (2019).

REFERENCES

- Valentina Alfi, Giorgio Parisi, and Luciano Pietronero. Conference registration: how people react to a deadline. *Nature Physics*, 3(11):746–746, 2007.
- Valentina Alfi, Andrea Gabrielli, and Luciano Pietronero. How people react to a deadline: time distribution of conference registrations and fee payments. *Open Physics*, 7(3):483–489, 2009.
- AMF. Study of the behaviour of high-frequency traders on Euronext Paris. 2017. Available at <https://www.amf-france.org/en/news-publications/publications/reports-research-and-analysis/study-behaviour-high-frequency-traders-uronext-paris>.
- Marco Avellaneda and Michael D. Lipkin. A market-induced mechanism for stock pinning. *Quantitative Finance*, 3(6):417, 2003.
- Marco Avellaneda, Gennady Kasyan, and Michael D. Lipkin. Mathematical models for stock pinning near option expiration dates. *Communications on Pure and Applied Mathematics*, 65(7):949–974, 2012.
- Michael Benzaquen and Jean-Philippe Bouchaud. Market impact with multi-timescale liquidity. *Quantitative Finance*, 18(11):1781–1790, 2018.
- Paul Besson and Raphaël Fernandez. Better trading at the close thanks to market impact models. 2021. Euronext quantitative research report.
- Blackrock. A global perspective on market-on-close activity. 2020. Available at <https://www.blackrock.com/corporate/literature/whitepaper/viewpoint-aglobal-perspective-on-market-on-close-activity-july-2020.pdf>.
- Jean-Philippe Bouchaud, Marc Mézard, and Marc Potters. Statistical properties of stock order books: empirical results and models. *Quantitative finance*, 2(4):251, 2002.
- Selma Boussetta, Laurence Daures-Lescourret, and Sophie Moinas. The role of pre-opening mechanisms in fragmented markets. In *Paris December 2017 Finance Meeting EUROFIDAI-AFFI*, 2017.
- Frédéric Bucci, Michael Benzaquen, Fabrizio Lillo, and Jean-Philippe Bouchaud. Crossover from linear to square-root market impact. *Physical review letters*, 122(10):108302, 2019.
- Eric Budish, Peter Cramton, and John Shim. The high-frequency trading arms race: Frequent batch auctions as a market design response. *The Quarterly Journal of Economics*, 130(4):1547–1621, 2015.

- Damien Challet. Strategic behaviour and indicative price diffusion in Paris Stock exchange auctions. In *New Perspectives and Challenges in Econophysics and Sociophysics*, pages 3–12. Springer, 2019.
- Damien Challet and Nikita Gourianov. Dynamical regularities of US equities opening and closing auctions. *Market microstructure and liquidity*, 4(01n02):1950001, 2018.
- Damien Challet and Robin Stinchcombe. Analyzing and modeling 1+ 1d markets. *Physica A: Statistical Mechanics and its Applications*, 300(1-2):285–299, 2001.
- Lorenzo Dall’Amico, Antoine Fosset, Jean-Philippe Bouchaud, and Michael Benzaquen. How does latent liquidity get revealed in the limit order book? *Journal of Statistical Mechanics: Theory and Experiment*, 2019(1):013404, 2019.
- Mike Derksen, Bas Kleijn, and Robin De Vilder. Clearing price distributions in call auctions. *Quantitative Finance*, 20(9):1475–1493, 2020.
- Mike Derksen, Bas Kleijn, and Robin De Vilder. Heavy tailed distributions in closing auctions. *Physica A: Statistical Mechanics and its Applications*, 593:126959, 2022.
- Jonathan Donier and Jean-Philippe Bouchaud. From Walras’ auctioneer to continuous time double auctions: A general dynamic theory of supply and demand. *Journal of Statistical Mechanics: Theory and Experiment*, 2016(12):123406, 2016.
- Jonathan Donier, Julius Bonart, Iacopo Mastromatteo, and Jean-Philippe Bouchaud. A fully consistent, minimal model for non-linear market impact. *Quantitative finance*, 15(7):1109–1121, 2015.
- Euronext. Euronext rule book, Book 1: Harmonised Rules. 2020. Available for download at <https://www.euronext.com/en/regulation/euronext-regulated-markets>.
- Narasimhan Jegadeesh and Yanbin Wu. Closing auctions: Nasdaq versus NYSE. *Journal of Financial Economics*, 143(3):1120–1139, 2022.
- Albert S. Kyle. Continuous auctions and insider trading. *Econometrica: Journal of the Econometric Society*, pages 1315–1335, 1985.
- Ismael Lemhadri. Price impact in a latent order book. *Market Microstructure and Liquidity*, 5(01n04):2050004, 2019.
- Fabrizio Lillo, J. Doyne Farmer, and Rosario N. Mantegna. Master curve for price-impact function. *Nature*, 421(6919):129–130, 2003.
- Iacopo Mastromatteo, Bence Toth, and Jean-Philippe Bouchaud. Agent-based models for latent liquidity and concave price impact. *Physical Review E*, 89(4):042805, 2014.
- Ioane Muni Toke. Exact and asymptotic solutions of the call auction problem. *Market microstructure and liquidity*, 1(01):1550001, 2015.
- Michael S. Pagano and Robert A. Schwartz. A closing call’s impact on market quality at Euronext Paris. *Journal of Financial Economics*, 68(3):439–484, 2003.
- Franck Raillon. The growing importance of the closing auction in share trading volumes. *Journal of Securities Operations & Custody*, 12(2):135–152, 2020.
- Bence Tóth, Yves Lempriere, Cyril Deremble, Joachim De Lataillade, Julien Kockelkoren, and Jean-Philippe Bouchaud. Anomalous price impact and the critical nature of liquidity in financial markets. *Physical Review X*, 1(2):021006, 2011.

Appendix A: Proof of Proposition 3

Proof. We only prove the proposition for an additional buy market order resulting in a price impact denoted by I_B . The case of a sell market order resulting in an impact I_S is symmetric. By definition, $\omega \mapsto p_\omega$ is a non-decreasing right-continuous step function; the same holds for $\omega \mapsto I(\omega)$. Obviously $I(0) = 0$ and $I(\omega) = 0$ if and only if $p_\omega = p_a$. Since $\omega^{(0)}$ denotes the first point of discontinuity of I , by monotonicity, the condition $p_\omega = p_a$ is equivalent to $\omega < \omega^{(0)}$. In the original auction \mathcal{A} with auction price p_a and auction volume Q_a , we have

$$\begin{cases} S(p_a) - V_S^R(p_a) = D(p_a) - V_B^R(p_a) = Q_a, \\ V_S^R(p_a) \times V_B^R(p_a) = 0. \end{cases} \quad (\text{A1})$$

All these quantities are fixed by the original auction setting. If we add a buy market order of size $q = \omega \times Q_a$ in this setting, the new auction price p_ω satisfies

$$\begin{cases} S(p_\omega) - V_S^R(\omega) = D(p_\omega) - V_B^R(\omega) + q, \\ V_S^R(\omega) \times V_B^R(\omega) = 0, \end{cases} \quad (\text{A2})$$

where S and D are the original supply and demand functions, and $V_S^R(\omega)$ (resp. $V_B^R(\omega)$) is the remaining sell quantity (resp. buy quantity) at price p_ω in the new setting. These volumes depend clearly on ω .

Let us now determine the first point of discontinuity $\omega_B^{(0)}$. It is clear that the first price change due to the addition of a market order of size $q = \omega_B^{(0)} Q_a$ occurs when $V_S^R(\omega) = V_S(p_\omega)$, $V_B^R(\omega) = 0$, and the new auction price $p_\omega = p_B^{(1)}$ is the first non empty price tick after p_a in the sense of $V_S + V_B$, i.e., the first tick price strictly greater than the auction price which contains buy or sell shares. (see Figure 1 to build an intuition). Equation (A2) yields

$$S(p_B^{(1)}) - V_S(p_B^{(1)}) = D(p_B^{(1)}) + q. \quad (\text{A3})$$

Using the fact that $S(p_B^{(1)}) = S(p_a) + V_S(p_B^{(1)})$ and $D(p_B^{(1)}) = D(p_a) - V_B(p_a)$ we obtain

$$S(p_a) = D(p_a) - V_B(p_a) + q, \quad (\text{A4})$$

hence, using equation (A1), one finds

$$V_S^R(p_a) = V_B^R(p_a) - V_B(p_a) + q. \quad (\text{A5})$$

Using $V_B(p_a) = V_B^R(p_a) + V_B^M(p_a)$, we obtain

$$q = V_S^R(p_a) + V_B^M(p_a), \quad (\text{A6})$$

which yields

$$\omega_B^{(0)} = \frac{1}{Q_a} (V_S^R(p_a) + V_B^M(p_a)) \quad (\text{A7})$$

Let us now determine $\omega_B^{(i)}$, $i \geq 1$: which is the $(i+1)^{\text{th}}$ point of discontinuity of I_B . We proceed similarly: the $(i+1)^{\text{th}}$ price change due to the injection of a market order occurs when $V_S^R(\omega) = V_S(p_\omega)$, $V_B^R(\omega) = 0$, and $p_\omega = p_B^{(i+1)}$ is the $(i+1)^{\text{th}}$ non empty price tick greater than p_a (in the sense of $V_S + V_B$). Equation (A2) yields

$$S(p_B^{(i+1)}) - V_S(p_B^{(i+1)}) = D(p_B^{(i+1)}) + q, \quad (\text{A8})$$

$$\sum_{p' < p_B^{(i+1)}} V_S(p') = \sum_{p' \geq p_B^{(i+1)}} V_B(p') + q, \quad (\text{A9})$$

$$S(p_a) + \sum_{p_a < p' < p_B^{(i+1)}} V_S(p') = D(p_a) - \sum_{p_a \leq p' < p_B^{(i+1)}} V_B(p') + q. \quad (\text{A10})$$

Using equation (A1), we obtain

$$Q_a + V_S^R(p_a) + \sum_{p_a < p' < p_B^{(i+1)}} V_S(p') = Q_a + V_B^R(p_a) - (V_B(p_a) + \sum_{p_a < p' < p_B^{(i+1)}} V_B(p')) + q. \quad (\text{A11})$$

Finally,

$$\sum_{p_a < p' < p_B^{(i+1)}} (V_S + V_B)(p') = q - (V_S^R(p_a) + V_B^M(p_a)). \quad (\text{A12})$$

Thus,

$$\omega_B^{(i)} = \omega_B^{(0)} + \frac{1}{Q_a} \sum_{p_a < p' < p_B^{(i+1)}} (V_S + V_B)(p') \quad , \quad i \geq 1, \quad (\text{A13})$$

which leads to

$$\omega_B^{(i)} = \omega_B^{(i-1)} + \frac{V_S(p_B^{(i)}) + V_B(p_B^{(i)})}{Q_a} \quad , \quad i \geq 1. \quad (\text{A14})$$

□

Appendix B: Proof of Proposition 4

Proof. Using Proposition 3 we have

$$\begin{aligned}
\omega_B^{(i)} - \omega_B^{(0)} &= \frac{1}{Q_a} \sum_{p_a < p' < p_B^{(i+1)}} V_S(p') + V_B(p') \\
&= \frac{1}{Q_a} \sum_{k=1}^i (V_S + V_B)(p_B^{(k)}) \\
&= \sum_{k=1}^i (p_B^{(k+1)} - p_B^{(k)}) (\tilde{\rho}_S + \tilde{\rho}_B)(p_B^{(k)}) \\
&= \tilde{\mathcal{L}}_B \sum_{k=1}^i (p_B^{(k+1)} - p_B^{(k)}) \\
&= \tilde{\mathcal{L}}_B (p_B^{(i+1)} - p_B^{(1)}) \\
&\approx \tilde{\mathcal{L}}_B p_B^{(1)} \left[I_B(\omega_B^{(i)}) - I_B(\omega_B^{(0)}) \right],
\end{aligned} \tag{B1}$$

where we used the approximation $I_B(\omega_B^{(i)}) - I_B(\omega_B^{(0)}) = \log(p_B^{(i+1)}/p_B^{(1)}) \approx p_B^{(i+1)}/p_B^{(1)} - 1$.

□